*Jurnal Mekanikal*
*June 2014, No 37, 64-80*

# SIMULATION OF COMBUSTION AND THERMAL FLOW IN AN INDUSTRIAL BOILER WITH NOx PREDICTIONS

Ruzita Aqmar Mohd Nordin, Muhd Noor Muhd Yunus[+] and Farid Nasir Ani

Faculty of Mechanical Engineering,
Universiti Teknologi Malaysia,
81200 Skudai, Johor DT, Malaysia
[+]Malaysian Nuclear Agency,
Bangi 43000, Kajang, Selangor, Malaysia

## ABSTRACT

*Disposal of municipal solid waste (MSW) is one of the major problems in many urban areas and can be considered a serious global environmental issue. Incineration has become the most environmental-friendly method of disposing waste and it is important for recovery of energy from waste which reduces the net release of carbon dioxide to the atmosphere and eliminates the production of methane from landfill. Computational fluid dynamics (CFD) modelling is used in the development phase and very useful tool for simulation modelling of the complex geometry and flow conditions in incinerators. CFD modelling and flow simulation with detailed parametric variations of design variables of an industrial scale MSW incinerator was done using ANSYS FLUENT to simulate the combustion and thermal flow and to determine velocity profiles, temperatures, and $NO_x$ distributions. In order to minimize the pollutants emission from the MSW incinerators, an improved mixing of air is formulated to increase oxidative destruction of incomplete combustion by secondary air injection into the combustion chamber. The results predicted that the $NO_x$ formation in the boiler is highly depended on the combustion processes along with the temperature and species concentrations. It has shown that over-fire air (OFA) operation is a good way to reduce the $NO_x$ emissions from the boiler.*

**Keywords :** *Combustion, $NO_x$ prediction, Computational Fluid Dynamics (CFD)*

## 1.0 INTRODUCTION

Municipal solid waste (MSW) is a major environmental problem faced by Malaysia. Statistically, the average production rates of MSW varied from 0.5–0.8 to 1.7 kg/person/day, (Kathirvale et al., 2003). The growing population and rapid development in Malaysia has given a big impact on MSW production which has increased from 5.6 million tonnes in 1997 to more than 8 million tonnes in 2010 with a projection of more than 9 million tonnes by 2020. The daily waste generation has also shown a rising trend. The MSW generation was 15,300 t/day in 1997 and predicted to reach 27,000 t/day by 2020 as presented with projection made for 2015 and 2020 as in Table 1, Zainura et al. (2013). Alternatively, Ismail and Ani (2013), predicted the daily generation of MSW in three highly populated states in Malaysia; Kuala Lumpur, Pulau Pinang, and Johor from 1996 to 2024 as presented in Figure 1. The predicted results from year 2014 and after is calculated using assumption and formula proposed by Saeed et al. (2008). The current disposal method in many countries is landfilling. Nevertheless, as populations grow, the need for landfill sites for other development purposes is increasing and this results in a dramatic decrease in availability of landfill sites. According to Ismail and Ani (2013), municipal landfills may be a way to manage waste, but it also contributes pollution such as contamination of groundwater and release of methane gas generated by decaying organic wastes.

Incineration has become the best option for an effective and economical way of waste disposal. Furthermore, it has the ability to reduce waste by up to 90% in volume and 75% in

*Corresponding author: farid@mail.fkm.utm.my

weight. Incineration also offers an opportunity for energy recovery. Energy recovery from incineration of MSW can be used to offset the difference in cost between incineration and other disposal techniques (Siritheerasas, 2008).

Table 1: Annual waste generation in Malaysia

| Year | Amount (tonnes) |
|---|---|
| 1997 | 5,600,000 |
| 1998 | 6,000,000 |
| 1999 | 6,105,000 |
| 2000 | 6,369,000 |
| 2005 | 6,970,000 |
| 2006 | 7,340,000 |
| 2007 | 7,655,000 |
| 2010 | 8,196,000 |
| 2015* | 9,111,000 |
| 2020* | 9,820,000 |

*Projected value
**Source : Zainura et al. (2013)

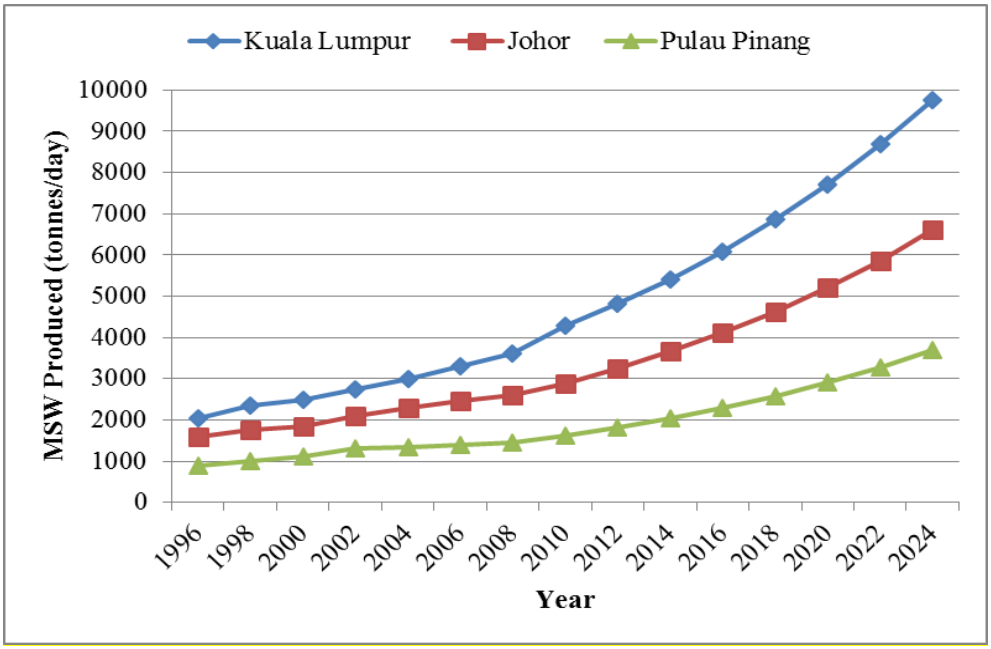


Figure 1: Daily MSW Generation in Malaysia

Composition of MSW can vary greatly due to inadequate current waste separation systems. Burning MSW with a wide variation in composition and high moisture content will lead to unstable combustion system, thus resulting in low combustion efficiency and releases unwanted pollutants such as CO and unburnt hydrocarbons. Therefore, a pre-treatment of MSW is performed to provide waste with more uniform composition and lower moisture content. Refuse-derived fuel (RDF) is an example of processed MSW which produced from a combustible fraction of MSW. Siritheerasas (2008) explained on the process which includes drying, shredding, and compacting waste into pellets. Advantages of RDF over un-processed MSW, RDF are more uniform in size and composition, lower moisture content, and higher heating value.

However, combustion always involves in pollutant formation and a source of destruction to the global environment. The species that evolves not only depend on the fuel

but also depend on the combustion conditions as such equivalence ratio, residence time, temperature, air supply. The combustion of MSW during the gaseous combustion phase has many stages such as moisture evaporation, waste devolatilization, combustion of volatiles, and mixing and fixed carbon combustion during heterogeneous chemical reactions (Kapitler, 2011).

In MSW combustion, the emissions of most concern are particularly NOx, HCl, chlorinated dioxins and furans. The formation of NOx in industrial boilers is a very complicated problem due to many parameters that influence its formation process. In order to make the boiler more efficient and less pollutant emission, it is important to understand the combustion and thermal flow behaviors inside the boiler. Ruth (1998) cited that four major classes of NOx control options can be applied to control NOx in MSW combustors. These are combustion zone control, selective non-catalytic reduction, selective catalytic reduction, and hybrid options that are combinations of the above.

Habib et al. (2010) mentioned that furnace average temperature and NO concentration decrease as the excess air factor increases for a given air mass flow rate. As the combustion air temperature increases, furnace temperature increases and the thermal NO concentration increases sharply. While Yin et al. (2008) cited that advanced secondary air supply system is one of the most important elements in the optimization of the gas combustion in the freeboard, for complete burnout and lower emissions. The secondary air can provide an effective combustion air, which prolongs the residence time of the combustibles, distributes the temperature more evenly, and leads to a better burnout.

Further study has been carried out using CFD simulation on the combustion process of the municipal waste incinerators. The work uses ANSYS workbench with Fluent as the software for obtaining the solution and post-processing to review the results. The simulation starts with design modeler to model the 2D incinerator. The meshing of the model was conducted by using ANSYS and the results have been processed by using FLUENT.

## 2.0 GOVERNING EQUATIONS

Computational fluid dynamics calculation and mathematical processes are governed by fluid flow governing equations. The equations are series of fluid properties which are conservation of mass, momentum, and energy, species, enthalpy, turbulent dissipation rate (κ) and turbulent dissipation rate (ε). It has been summarized as follows;

i. Conservation of Mass (Continuity Equation):

$$\frac{\partial \rho}{\partial t} + \nabla . \rho U = 0 \tag{1}$$

ii. Conservation of Momentum (Momentum Equation):

$$\frac{\partial \rho U}{\partial t} + (\nabla . \rho UU) = -\nabla p + \nabla . \tau + \rho g \tag{2}$$

iii. Conservation of Energy (Temperature):

$$\rho c_p \frac{DT}{Dt} = \nabla . \lambda_e \nabla T - \nabla . \Sigma_l \rho h_l(T) D_e \nabla m_l - \rho \Sigma_l \frac{D m_l}{Dt} h_l(T) \tag{3}$$

iv. Enthalpy:

$$\rho c_p \frac{DT}{Dt} = \nabla . \lambda_e \nabla T - \nabla . q_{rad} + \nabla . \Sigma_l \rho h_l(T) D_e \nabla m_l \tag{4}$$

v. Species Mass Fraction:

$$\frac{\partial \rho m_l}{\partial t} + \nabla . \rho U m_l = \nabla . D_e \rho \nabla m_l - R_l \tag{5}$$

As for turbulent model, κ-ε model is practical for many flows and relatively simple to implement and easy to converge. The equation for;

Turbulent kinetic energy (κ):

$$\frac{\partial}{\partial t}(\rho\kappa) + \frac{\partial}{\partial x_i}(\rho\kappa u_i) = \frac{\partial}{\partial x_j}\left[(\mu + \frac{\mu_t}{\sigma_\kappa})\frac{\partial \kappa}{\partial x_j}\right] + P_\kappa + P_b - \rho\varepsilon - Y_M + S_\kappa \quad (6)$$

Turbulent dissipation rate (ε)

$$\frac{\partial}{\partial t}(\rho\varepsilon) + \frac{\partial}{\partial x_i}(\rho\varepsilon u_i) = \frac{\partial}{\partial x_j}\left[(\mu + \frac{\mu_t}{\sigma_\varepsilon})\frac{\partial \varepsilon}{\partial x_j}\right] + C_{1\varepsilon}\frac{\varepsilon}{\kappa}(P_k + C_{3\varepsilon}P_b) - \rho C_{2\varepsilon}\frac{\varepsilon^2}{\kappa} + S_K \quad (7)$$

where;

Turbulent viscosity, $\mu_t$

$$\mu_t = \rho C_\mu \frac{\kappa^2}{\varepsilon} \quad (8)$$

Production of κ, $P_\kappa$

$$P_\kappa = -\overline{\rho u_i' u_j'}\frac{\partial u_j}{\partial x_i} \quad (9)$$

Effect of buoyancy, $P_b$

$$P_b = \beta g_i \frac{\mu_t}{Pr_t}\frac{\partial T}{\partial x_i} \quad (10)$$

where;

$$\beta = -\frac{1}{\rho}\left(\frac{\partial \rho}{\partial T}\right)p \quad (11)$$

While $g_i$ component of gravitational factor. Turbulent Prandtl number, Pr is 0.85 are suitable for both standard and realizable κ-ε model. Other model constants are $C_{1s}$, $C_{2s}$, $C_{3s}$, $C_\mu$, $\sigma_k$ and $\sigma_\varepsilon$.

## 3.0 METHODOLOGY

CFD is one of the methods to virtually design and run the simulation without the need to physically build the model. An established CFD computational program, ANSYS FLUENT, have been chosen to carry out the simulation for this study. This software is a leading CFD application from ANSYS and it widely used in almost every industry sector and manufactured product. Especially for newly develop model, the computational testing using Computational Fluid Dynamics (CFD) software will reduce a lot of trial and error on experimental work.

The CFD study is focused on developing the simulation of combustion in the studied industrial boiler. The simulation was carried out using ANSYS 14.5. The ANSYS Modeler was used to model the combustor and ANSYS Meshing was used to mesh the model. Finally, FLUENT was used to obtain the solution. Later, the post-processing was carried out using CFD-Post. The non-premixed combustion with turbulent realizable κ-ε was used in the simulation of combustion in the combustion chamber. In this paper, the simulation work was carried out based on actual industrial RDF boiler, located in Semenyih, Malaysia. The boiler is equipped with rotary feeders and pneumatic spreaders to feed the RDF into the furnace. Fuel is partially burned in suspension and further the combustion takes place on the chain grates stocker where most of solid particle are burned. The furnace has a single-pass radiation heat transfer zone with gooseneck arches at the secondary combustion zone and the inlet to the superheater.

Fuel on the grate with 70% volatiles burning with primary air in a reduction zone at a temperature of less than 650°C releases the volatiles, which move up to the secondary combustion zone for complete combustion with minimum formation of nitrogen oxides. The wind box supplying primary air is classified along the length of the grate with individual dampers to enable effective control of fuel combustion on the grate. The volatiles and lighter

elements of fuel that float in the secondary combustion zone when injected by the spreaders are subjected to the turbulent secondary air jets for the combustion to take place. A complete combustion is ensured with 30% excess air in oxidizing zone. The flue gas passes through a dust collector for removing fly ash and a wet scrubber for neutralizing acid gases. The model was simplified and modelled using ANSYS and later by FLUENT for further analysis. The design parameters are listed in Table 2.

Table 2: Design Parameter of the RDF Boiler

| | **Parameter** | **Value** |
|---|---|---|
| 1 | Boiler Dimension (L x W x H) | 5.3m x 4.9m x 23m |
| 2 | Primary Air Inlet Velocity (m/s) | 30 |
| 3 | Secondary Air Inlet Velocity (m/s) | 12 |
| 4 | RDF Fuel Velocity (m/s) | 0.5 |
| 5 | RDF Fuel Temperature (K) | 300 |

Prior to solving the model, geometry is discretized into grids. Model meshing is the most critical part of the CFD process. The quality of mesh is determined by the technique selected during meshing. Meshing creates grid of cells or elements which fluid flow equations are able to be solved (Figure 2). In this study, ANSYS Meshing is used to generate required grids. The grid is conducted by 2 types of mesh; coarse and fine mesh. However, a relatively coarse grid of 12,602 cells was used, consisting of all hexahedral elements. This grid is selected due to it is compromise by getting a fine resolution of the flow details and minimizing the computer time needed to complete the simulations.

Nonetheless, with the use of a more refined grid, it is require having smaller time steps, more number of iterations per time step and four times more calculation per iteration for the solution to converge. It is very important to use a grid that is independent of the solution and that is finer where the gradients of the main parameters are critical. The setting parameters for meshing that has been adapted for this simulation are shown in Table 3.

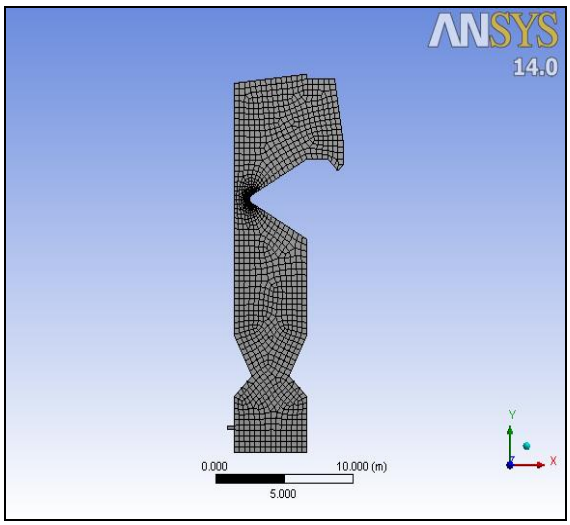


Figure 2: 2D Meshing

The boundary conditions are specified according to the geometric arrangement of the boiler. The boundary conditions on the surface geometry have been assigned by FLUENT for the 2D model which consists of RDF inlet, primary air inlet, secondary air inlet, wall and outlet which are shown in Figure 3. For this simulation, it is assumed that methane gas was used as a fuel to substitute the RDF fuel. There are four inlets for the secondary air inlet which are located at the gooseneck of the boiler.

Table 3: Meshing Sizing Parameter

| SIZING PARAMETER | SETTING |
|---|---|
| Advance Size Parameter | Proximity and Curvature |
| Relevance Centre | Coarse |
| Initial Size Seed | Active Assembly |
| Smoothing | High |
| Transition | Slow |
| Span Angle Centre | Fine |
| Curvature Normal Angle | Default ( 18.0º ) |
| Proximity Min Size | 0.5 |
| Number Cells Across Gap | Default (3) |
| Min Size | Default (0.35665 mm) |
| Proximity Min Size | Default (0.35665 mm) |
| Max Face Size | Default (35.665 mm) |
| Max Size | Default (71.3290 mm) |
| Growth Rate | Default (1.20) |
| Minimum | 1.2 mm |

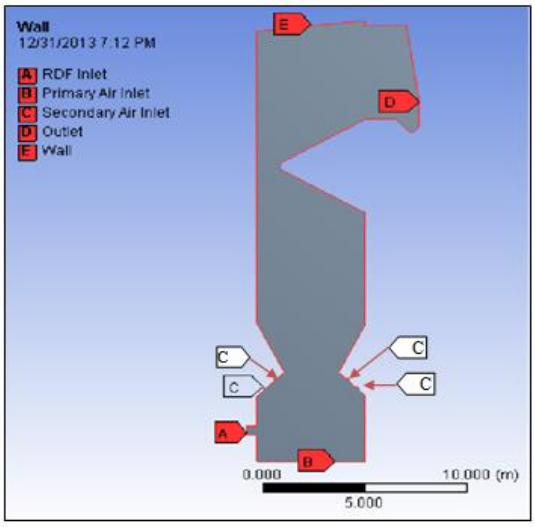


Figure 3: Boundary Conditions on 2D model

The procedures for performing the simulation in ANSYS FLUENT 14.0 are as showed in the flowchart in Figure 4.

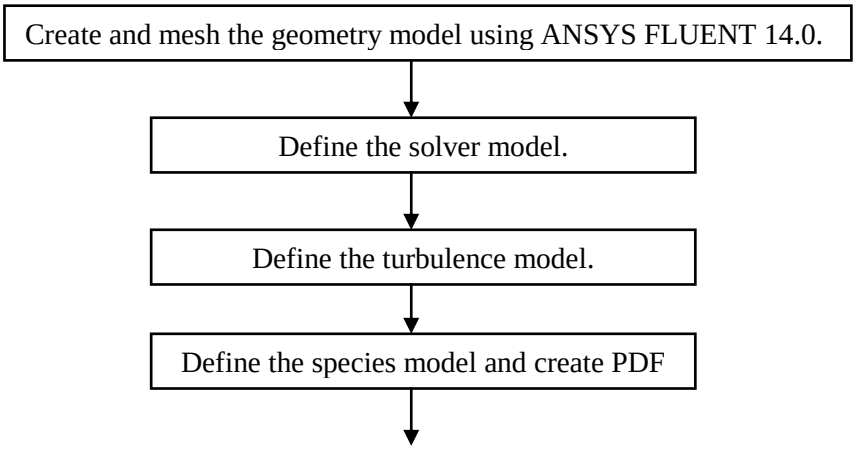

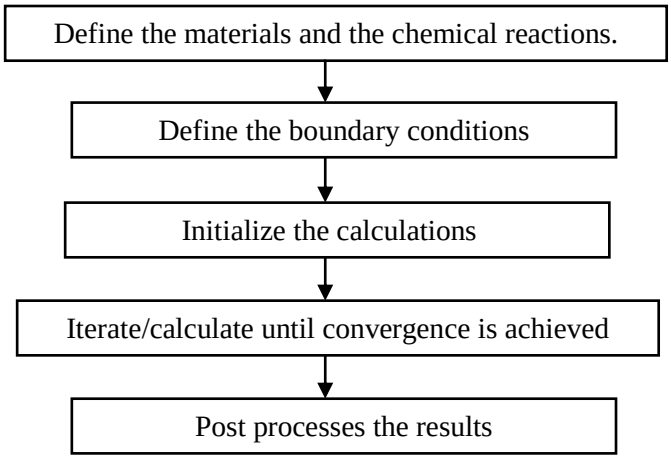


Figure 4 : Procedures for Performing the Simulation in ANSYS FLUENT 14.0

Simulation was carried out using the commercial CFD code ANSYS FLUENT 14.0. This study has been carried out with initial setting using transient time, 2-dimensional with pressure-based type solver. A few assumptions are made during the simulation of the studied boiler. It has been assumed that the process is simulated by using methane gas, $CH_4$ as the boiler fuel. The fuel was created by the mixing of methane (60%) and carbon dioxide (40%) on molar basis. For the oxidant, the mixing of nitrogen (79%) and oxygen (21%) was use as the normal combustion air configuration.

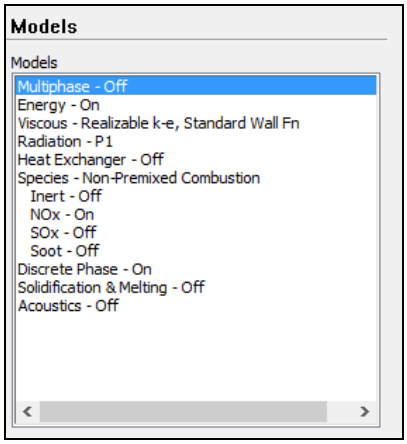


Figure 5: Model Setting in FLUENT

Model has been used were Langrangian Model including κ-ε equation. The detail of model parameter setting is shown in Figure 5. The flow is defined as turbulent, thus realizable κ-ε model is suitable to be applied. Under species model, Non-Premixed Combustion is selected. Automatically, FLUENT will request the input of the PDF file to be used in the simulation. By selecting and read data in Figure 6, the non-adiabatic PDF file, FLUENT reports that a new material, called pdf-mixture, has been created and defined in pre-PDF and their thermodynamic properties. The P-1 model is being used as it is one of the radiation models that can account for the exchange of radiation between gas and particulates. Simulations were carried out with time step $1e^{-3}$ s.

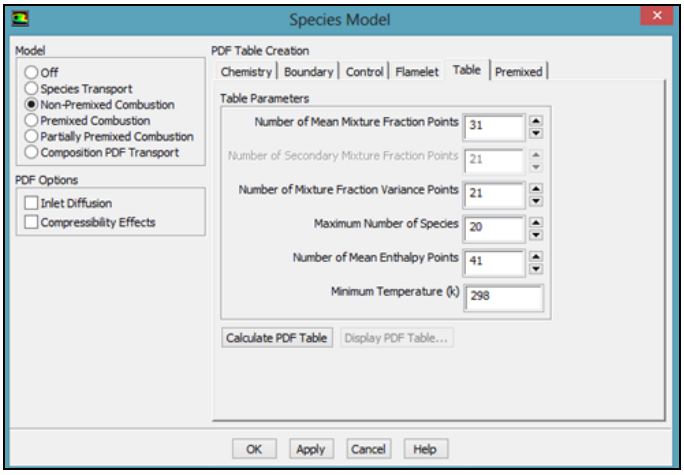


Figure 6: Species Model with PDF Table Parameter

The SIMPLE and second order upwind scheme was employed for the spatial discretization of the continuity, momentum, turbulent kinetic energy and turbulent dissipation rate equations while time was discretized using first order implicit. The solution method parameter settings are listed as in Table 5. The governing equations of mass and momentum conservation as well as the temperature equation are solved by using the method of finite volume.

Table 4: Simulation Parameter

| **Parameter** | **Value** |
|---|---|
| Fuel | Methane |
| Fuel Flow Rate (kg/s) | 3.89 |
| Fuel Temperature (K) | 300 |
| Primary Air Flow Rate (kg/s) | 16.6 |
| Primary Air Temperature (K) | 1650, 1750 |
| Secondary Air Flow Rate (kg/s) | 13.6 |
| Operating pressure (Pa) | 101325 |
| Gravitational Acceleration ($m/s^2$) | 9.81 |
| Time Step (s) | 0.001 |

Table 5: Solution Method Parameter Setting

| **No.** | **Solution Method Parameter** | **Setting** |
|---|---|---|
| 1 | Pressure-Velocity-Coupling | SIMPLE |
| 2 | Gradient | Least Squares Cell Based |
| 3 | Pressure | Standard |
| 4 | Momentum | Second Order Upwind |
| 5 | Turbulent Kinetic Energy | Second Order Upwind |
| 6 | Turbulent Dissipation Rate | Second Order Upwind |
| 7 | Pollutant No | Second Order Upwind |
| 8 | Energy | Second Order Upwind |
| 9 | Discrete Ordinates | Second Order Upwind |
| 10 | Mean Mixture Fraction | Second Order Upwind |
| 11 | Mixture Fraction Variance | Second Order Upwind |
| 12 | Transient Formulation | First Order Implicit |

The case need to be checked to ensure no error before it started and the model are ready to be simulated. The check case is checking the mesh, models, boundaries and cell zone, materials and solver. In this simulation, the calculation was setup up to 9000 iterations and the calculation was converged and result was satisfied with non-premixed combustion in an industrial boiler as expected as shown in Figure 7.

The convergence of the solution is very important to ensure the end result of simulation is correct and accurate. The relaxation method may be used to speed up or delay the solution by using the relaxation factor. The most sensitive relaxation factor for the combustion simulation is energy, temperature, radiation and mean mixture fraction (Noor et al., 2013).

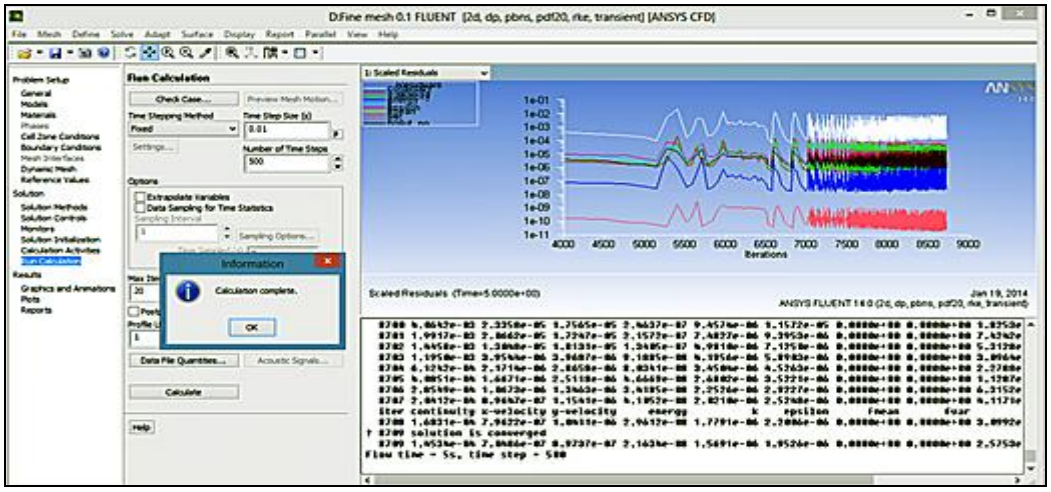


Figure 7: Converged solution

## 4.0 RESULTS AND DISCUSSION

Data need to be collected to be inserted into the algorithm generated to generate desired result. The data gathered through actual performance of studied boiler. Later, the analysed data are used to generate the simulation. The results obtained are verified for correctness and accuracy. The accuracy of the results generated by the ANSYS FLUENT will be verified by comparison with the previous study.

In order to ensure the accuracy, the grid sensitivity test was carried out to validate the CFD results that are self-governing from the mesh size. The simulations were performed by 2 types of mesh which are coarse mesh (53 x 238) and fine mesh (106 x 472). The computed solid volume fraction different grid sizes (x or y axis) are plotted. It seems it can be concluded that for both fine mesh (50,002) and coarse mesh (12,602) as shown in Figure 8.

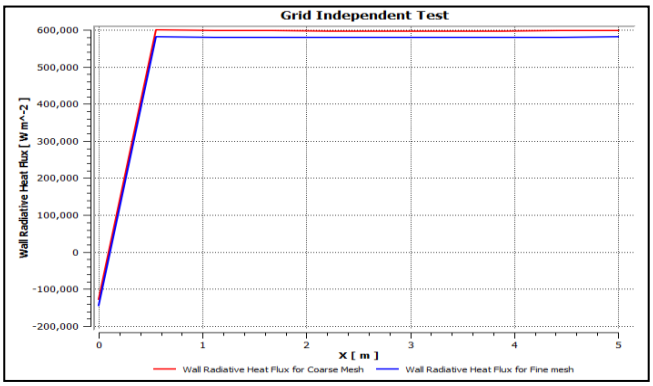


Figure 8: Grid Sensitivity Test

### 4.1 Validation of the Combustion Simulation Results

In order to achieve a stable calculations and fast convergences for two-phase flow, combustion, heat-transfer and chemical reactions, first, the gas flow equations need to be solved. After the flow field converges, the particle trajectories interacting with the flue gas are calculated. Then, the chemical reaction and enthalpy equations for combustion are taken into account. Numerical calculations are repeated until the flow and temperature convergence is reached. $NO_x$ transport equations later are solved based on the predicted flow and temperature. A convergence criterion is the normalized residuals for variables need to be less than $10^{-3}$. Flow and temperature field convergence is obtained after more than 20,000 iterations. The $NO_x$ calculation requires smaller iterations with a total of approximately 300 times.

The results predicted from the numerical calculations are then compared with the design values at the boiler exit. The comparison between the measured values and predicted results shows good agreement. The predicted $NO_x$ emissions at the boiler exit are 330 $mg/Nm^3$, respectively. The flow profiles, temperature and $NO_x$ emissions are featured in the following sections, have shown a consistent results with the previous studies (Choi and Kim, 2009), (Diez et al., 2008). This means that the adopted numerical models in the present calculations are reasonable for combustion analysis and $NO_x$ prediction in the boiler.

### 4.2 Velocity Flow Profiles and Distributions

The velocity distribution and contours inside the boiler height are shown in Figure 9. The flows located near the burners show more turbulence than in other locations. A swirling flow formed via the air and fuel particles injected through the burner ports is found in the center of the boiler, as expected. The swirling flow is stronger in the lower level than in the higher level. In the upper region, the swirling flow is remarkably reduced.

The flue gas flows into the primary superheater with upward velocity distribution located downstream, after the boiler exit, is relatively flat and the swirling flow is very weak. This implies that superheater and reheater installed downstream help the flow to be even and the residual swirling flow to be reduced.

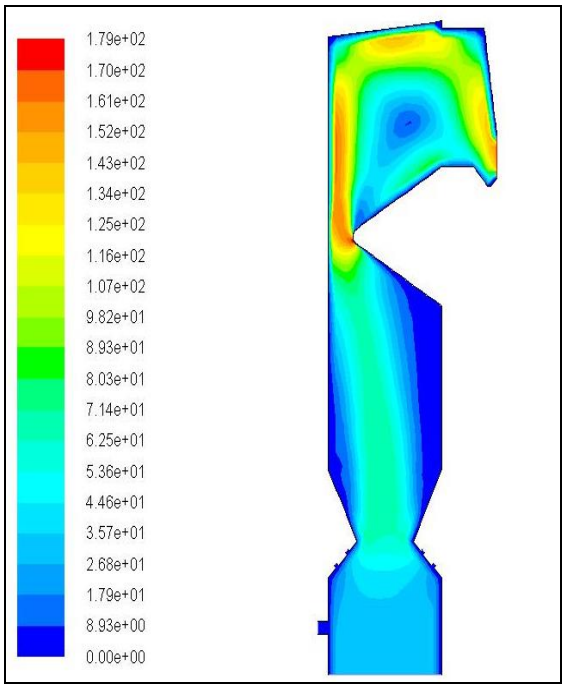


Figure 9: Velocity contour inside the boiler

The streamlines of the flue gas are depicted in Figure 10. The fuel particle trajectories are very similar to the flue gas pathlines but not coincident due to the different densities and turbulent fluctuations. The flue gas and fuel particles injected from the lower burners initially circulate in the bottom of the boiler and the ash hopper, and eventually travel up through the high-temperature and swirling-flow region formed in the central region of the boiler.

Devolatilization and char combustion take place while the fuel particles are traveling around the boiler. In general, it is known that all fuel species except char are consumed very quickly in the boiler. However, char burns at a slower rate and being consumed in the central region of the boiler. In this calculation, the conversion ratio of the combusting particles is approximately complete combustion. This implies that the present combustion processes offer sufficient residence time even for char conversion.

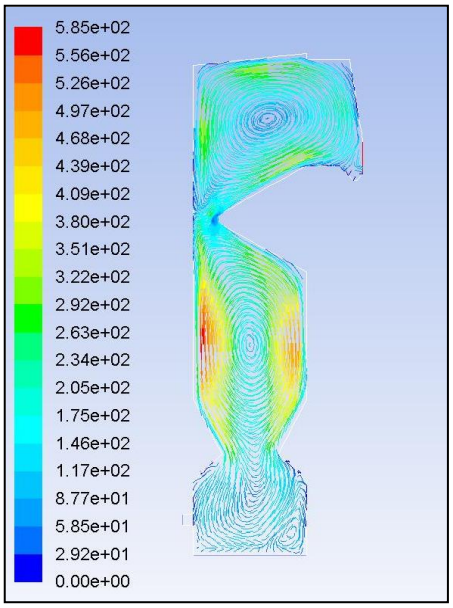


Figure 10: Velocity magnitude profiles inside the boiler

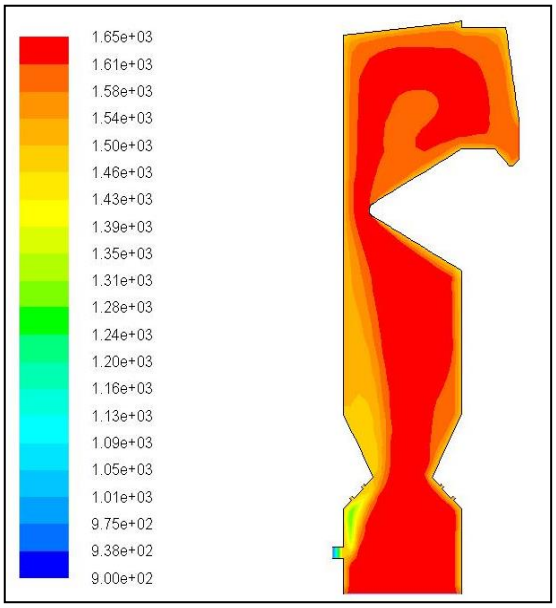


Figure 11: Temperature contour inside the boiler

### 4.3 Temperature Distributions

The temperature distributions in the boiler are shown in Figure 11. The temperature of the flue gas is relatively high in the central region of the boiler where combustion actively takes place. As the flue gas flows from the boiler exit to the boiler exit, the temperature gradually decreases due to the heat transfer from the flue gas to the boiler walls, reheater, superheater and economizer. The temperature of the air injected from the primary air inlet is 900K, and it increases up to a maximum temperature of 1650 K in the central region of the boiler. A notable temperature deviation is seen in the lower level of the boiler, but in the higher levels, the temperature deviation decreases due to stronger swirling and increased mixing.

With the increased height, the average temperatures also increase because of high combustion intensity. However, as the flue gas goes upward in the boiler, the temperature of the flue gas decreases due to the heat transfer between the flue gas and boiler walls via convection and radiation. Finally, the flue gas leaves the boiler at an average temperature of 700 K. The high temperature regions are closely related to thermal $NO_x$ formation which is dependent on local temperature. In this study, the temperature difference of air injected at the primary inlet has been study to determine the velocity profiles between the different values. It has been carried out for temperature 1650 K and 1750 K. The parameter for this study has been listed in Table 6.

Table 6: Parameter for Case Study Simulation

| Parameter | Velocity (m/s) | Case 1 | Case 2 |
|---|---|---|---|
| | | Temperature (K) | Temperature (K) |
| RDF Fuel | 2 | 300 | 300 |
| Primary Air | 30 | 1650 | 1750 |
| Secondary Air | 12 | 1500 | 1500 |
| Outlet | - | 2000 | 2000 |
| Wall | - | 700 | 700 |

The velocity profiles and temperature field difference can be visualized as shown in Figure 12 and 13.

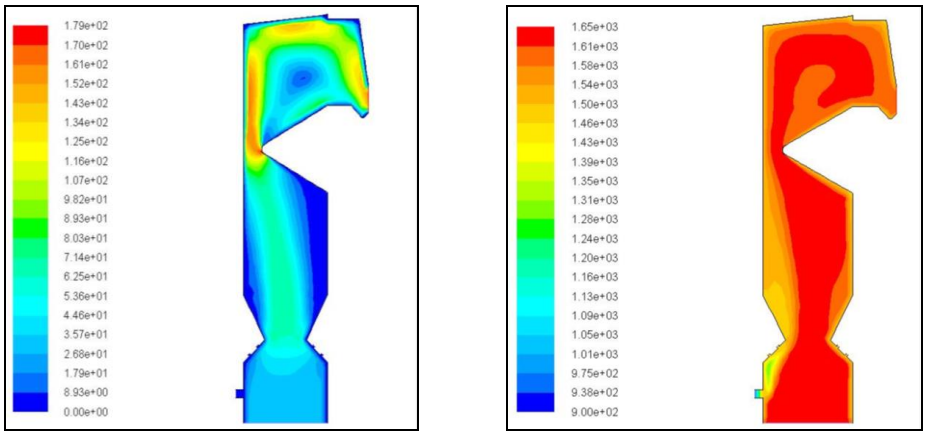


(a) (b)

Figure 12: Contours for Case 1; (a) Contour of velocity magnitude (m/s), (b) Contour of static temperature (K)

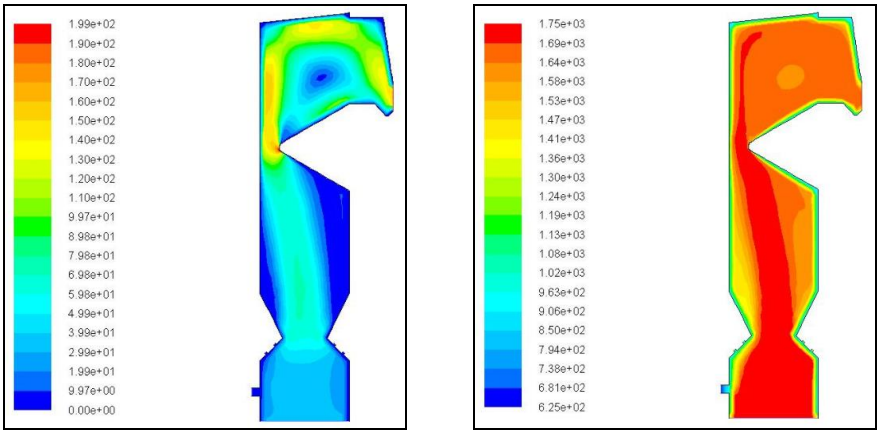


(a) (b)

Figure 13: Contours for Case 2; (a) Contour of velocity magnitude (m/s), (b) Contour of static temperature (K)

The change pattern of the flue gas temperature is clearly shown along the boiler height which gives effect on the velocity profile. According to simulations, the temperature is high in the area near to the primary air inlet, but as the flow of particles moves towards the freeboard area to the exit, the combustion process has slow down and temperature decrease. Most of the combustible material in waste is burned in the bed and its immediately adjacent freeboard region, producing carbon dioxide ($CO_2$) and water ($H_2O$) (Hussain et al., 2006).

### 4.4 Effects of the Secondary Air on Flow

The function of secondary air or overfire air (OFA) injection in fired boilers is primarily for CO and $NO_x$ removal. The secondary air jet curtains also serve to interact with the main flame column generated by the RDF injection spreaders to move the flame pattern, increase fuel–air mixing and reduce unburnt fuel particle from the boiler.

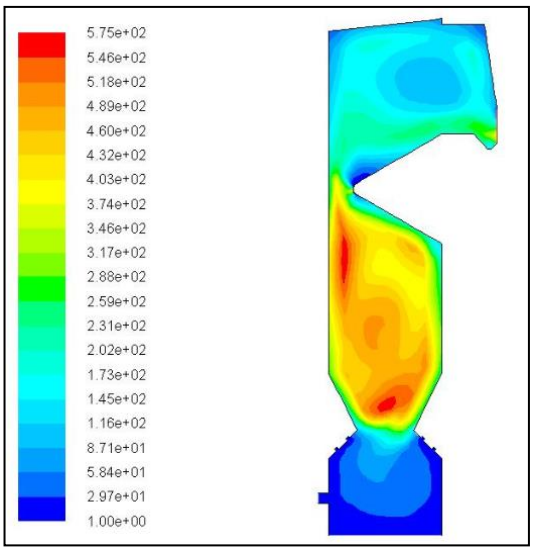


Figure 14: Contours of Turbulent Kinetic Energy (k) with Secondary Air

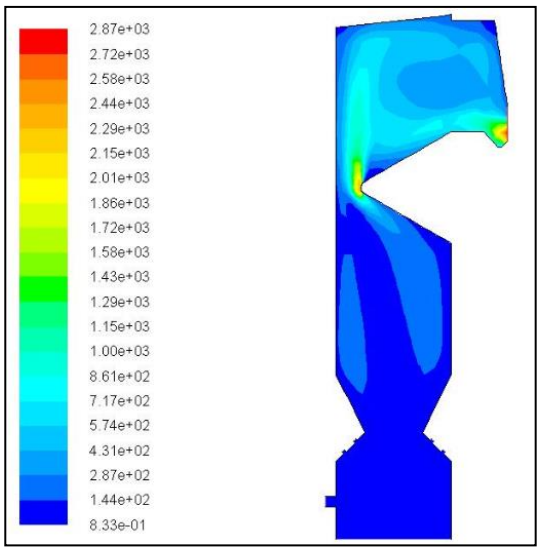


Figure 15: Contours of Turbulent Kinetic Energy (k) without Secondary Air

The conventional secondary air and spreader flow pattern as shown in Figure 14 generates a predominant upflow column positioned towards the rear centre of the boiler. There may be a low strength recirculation flow adjacent to the boiler front wall. The trajectory of the fuel particles through the boiler space, which eventually determines the residence time for burnout, is vertically upward with a small flow deflection around the nose at the boiler exit ahead of the superheater section.

From the simulation, it is shown that with the appearance of secondary air, it gives a turbulence effect at the centre of the boiler compared to the boiler without the supply of the secondary air. The existence of secondary air also increase the operating efficiency of the retrofitted boiler attained 73−75% and the unburned carbon in fly ash was less than 5% which also leads to reduction of $NO_x$ emission (Sun et al., 2012). The improvement of air supply systems and optimized grate systems can significantly enhance the mixing, reduce the excess air, improve the combustion process, and decrease the pollutants emission.

### 4.5 $NO_x$ Emissions

The $NO_x$ concentration contour showing a $NO_x$ concentration zone of 330 mg/Nm$^3$ are depicted in Figure 16. The predicted maximum $NO_x$ concentration is 353 mg/Nm$^3$ and the relatively high $NO_x$ concentration zones are found in the furnace center where the temperature is higher and the combustion processes are more active. The results show that the $NO_x$ emission is fairly low due to the combination of the use of staging combustion technology.

Since fuel and thermal $NO_x$ formation rates primarily depend on the temperature and fuel/oxygen ratio within the combustion region, $NO_x$ is mostly formed within an envelope of flames. Near the burner region, the rapid release of the volatiles contained in the coal, along with the incoming $O_2$ injected from the burners, lead to the rapid formation of HCN or $NH_3$.

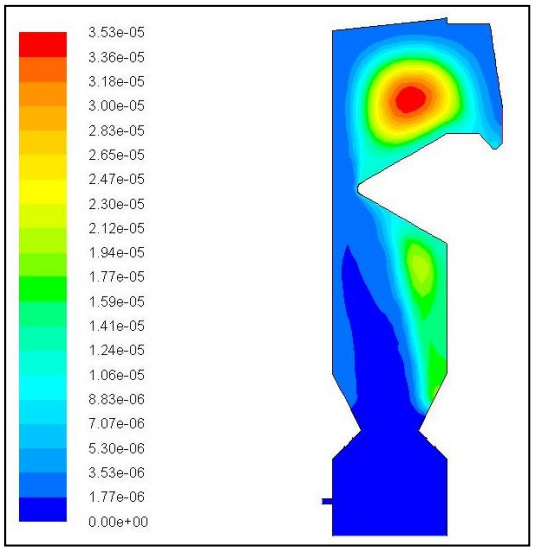


Figure 16: Contours of Mass Fraction of $NO_x$

A fraction of the N contained in the formed HCN and $NH_3$ is converted to NO in fuel-lean regions and $N_2$ in fuel-rich regions. The zones with a high thermal $NO_x$ formation rate are found within the high temperature regions when compared to the temperature and $O_2$ mass fraction distributions shows the zones of the total $NO_x$ formation. The total $NO_x$ formation region is not the same as the combined region for the thermal and fuel $NO_x$ formation. This difference is caused by reversible reactions where the $NO_x$ that is formed by a reaction mechanism is destroyed in other reaction mechanism.

As discussed above, these results show that majority of $NO_x$ is formed within the frame envelope. The $NO_x$ formation rates are low since the oxygen concentration is very low in the central zones, although the temperature is relatively high. The sources of intermediates (HCN and $NH_3$) from the volatiles and the source of NO from the char depend on the burnout and devolatilization rates. These results show that the $NO_x$ formation in the boiler depends on considerably on combustion processes such as burnout and devolatilization as well as temperature and species concentrations.

## 5.0 CONCLUSIONS

This work presents the simulation of combustion and thermal flow in industrial boiler and the prediction of $NO_x$ emission. It also determines the velocity profiles and temperatures inside the boiler. The characteristics of the flow, combustion, temperature and $NO_x$ emissions in the industrial boiler have been numerically investigated using comprehensive models for the combustion processes and $NO_x$ formation. Accurate predictions need attentions in selecting the calculation domain, generating mesh, and choosing numerical models, since $NO_x$ formation is affected by fluid flow, temperature and oxygen concentration distributions.

The flow fields, flue gas, temperature distributions, species distributions and $NO_x$ emissions in the boiler have been obtained and compared with the measured values. The comparison between the predicted results and measured values has shown a good agreement. It implies the adopted combustion and $NO_x$ formation models are suitable for predicting the characteristics of the flow, combustion, temperature and $NO_x$ emissions in the boiler. The predicted results have shown that the $NO_x$ formation in the boiler highly depended on the combustion processes along with the temperature and species concentrations. From the results obtained by this study, it has shown that over-fire air (OFA) operation is a good way to reduce the $NO_x$ emissions from the boiler.

The decrease in the fuel $NO_x$ formation is due to the low interaction of nitrogen from the fuel with oxygen in the combustion air. However the decrease in thermal $NO_x$ formation is caused by the decrease in temperature. It is generally accepted that at temperatures below 1800 K, thermal $NO_x$ is not significantly formed by the Zeldovich mechanism and is also not a major source of $NO_x$ in local fuel-rich zones. Therefore, for more accurate control of $NO_x$ formation, it is important to control temperatures above 1,800 K and encourage fuel-rich conditions.

## ACKNOWLEDGEMENTS

The authors wish to thank Universiti Teknologi Malaysia and the Malaysian Nuclear Agency (MNA) for supporting this research activities.

## REFERENCES

Abdul, A., Rozainee, M. Anwar, J and Wan Alwi, R.S, 2011. Combustion Studies of Refused-Derived Fuel (RDF) in Fluidized Bed (FB) System a Method. *2011 IEEE First Conference on Clean Energy and Technology CET. 978-1-4577-1354-5/11 2011*.

Ahmad Hussain, Farid Nasir Ani, Norzalia Sulaiman and Mohammed Fadzil Adnan, 2006. Combustion modelling of an industrial municipal waste combustor in Malaysia. *International Journal of Environmental Studies, 63(3),* 313–329.

ANSYS-INC. (2011). *ANSYS FLUENT User's Guide*. Release 14.0.

ANSYS-INC. (2011). *ANSYS FLUENT Theory Guide*. Release 14.0.

ANSYS-INC. (2011). *ANSYS FLUENT Tutorial Guide*. Release 14.0.

Chang Kook Ryu and Sangmin Choi, 1996. 3-Dimensional Simulation of Air Mixing in the MSW Incinerators. *Combustion Science and Technology,119,* 155-170.

Chen, S.S., Isnazunita Ismail, Abdul Nasir Adnan, Puvaneswari Ramasamy, 2011. Refuse Derived Fuel – Case Study of Waste as Renewable Resource. *International Journal for Sustainable Innovations, 1(1).*

Choeng Ryul Choi, Chang Nyung Kim, 2009. Numerical Investigation on the Flow, Combustion and NOx Emission Characteristics in a 500 MWe Tangentially Fired Pulverized-Coal Boiler. *Fuel 88,* 1720–1731.

Chungen Yin, Lasse A. Rosendahl, Søren K. Kær, 2008. Grate-firing of Biomass for Heat and Power Production. *Progress in Energy and Combustion Science 34,* 725– 754.

Dixon, T.F., Mann, A.P., Plaza, F. and Gilfillan, W.N., 2005. Development of Advanced Technology for Biomass Combustion—CFD as an Essential Tool. *Fuel 84,* 1303–1311.

Donghoon Shin and Sangmin Choi, 2000. The Combustion of Simulated Waste Particles in a Fixed Bed. *Combustion and Flame 121*,167–180.

Eddy H. Chui and Haining Gao, 2010. Estimation of NOx Emissions from Coal-Fired Utility Boiler. *Fuel 89,* 2977-2984.

Gittinger J.S., Arvan W.J., 1998. Considerations for the Design of RDF-Fired Refuse Boilers. *Power-Gen Europe '98, June 9-11, 1998,* Milan, Italy.

Habib M.A., Elshafei M., 2006. *Computer Simulation of NOx Formation in Boilers.*

Habib M.A., R. Ben-Mansour and Abualhamayel H.I., 2010. Thermal and Emission Characteristics in a Tangentially Fired Boiler Model Furnace. *Int. J. Energy Resource, 34,* 1164–1182.

Habib M.A., Elshafei M., Dajani M., 2008. Influence of Combustion Parameters on NOx production in an Industrial Boiler. *Computer & Fluids 37,* 12-23.

Ismail N and Ani FN, 2013. Solid Waste Management and Treatment in Malaysia. *Applied Mechanics and Materials.*

Kathirvale S, Muhd Yunus MN, Sopian K, Samsuddin AH, 2003. Energy Potential from Municipal Solid Waste in Malaysia. *Renewable Energy 29,* 559–67.

Kitto J.B. and Stultz S.C., 2005. *Steam/ Its Generation and Use, Chapter 29: Waste-to-Energy Installations*. 41st Edition. Babcock and Wilcox Company.

Lawrence A. Ruth, 1998. Energy from Municipal Solid Waste: A Comparison with Coal Combustion Technology. Prog. *Energy Combust. Sci.,24,* 545-564.

Ligang Liang, Rui Sun, Jun Fei, Shaohua Wu, Xiang Liu, Kui Dai, Na Yao, 2008. Experimental study on effects of moisture content on combustion characteristics of simulated municipal solid wastes in a fixed bed. *Bioresource Technology, 99,* 7238–7246.

Luis I. Diez, Cristobal Cortes, Javier Pallares, 2008. Numerical Investigation of NOx Emissions from a Tangentially-Fired Utility Boiler Under Conventional and Overfire Air Operation. *Fuel 87,* 1259–1269.

Mel Fox and Ande L.Boehman, 2004. Simulation and NOx Corelation for Coal-Fired Boiler. Prepr. Pap. –Am. Chem. Soc., Div. *Fuel Chem, 49 (2),* 824.

Minghou Xu, Azevedo, J.L.T and Carvalho, M.G., 2001. Modelling of a Front Wall Fired Utility Boiler for Different Operating Conditions. *Comput. Methods Appl. Mech. Engrg., 190,* 3581-3590.

Miran Kapitler, Niko Samec, and Filip Kokalj, 2011. Computational Fluid Dynamics Calculations of Waste-To-Energy Plant Combustion Characteristics. *Thermal Science, 15(1),* 1-16.

Nasserzadeh, V., Swithenbank, J., Scott, D. and Jones, B., 1991. Design Optimization of a Large Municipal Solid Waste Incinerator. *Waste Management, 11,* 249-261.

Noor, M.M, Andrew P. Wandel and Talal Yusaf, 2013. Detail Guide for CFD on the Simulation of Biogas Combustion of Biogas Combustion in Bluff-Body MILD Burner. *ICMER 2013, Kuantan, Malaysia. 1-3 July, Paper ID: P342.*

Prodpran T. Siritheerasas, Panitta Sawasdee, and Sudtida Inthakanok, 2008. Combustion of a Single-particle Refuse-derived Fuel (RDF). *Thammasat Int. J. Sc. Tech, 13 Special Edition.*

Raja Sarapalli, Ting Wang, Benjamin Day, 2005. Simulation of Combustion and Thermal Flow in an Industrial Boiler. *Proceedings of 27th Industrial Energy Technology Conference. May 11-12, 2005,* New Orleans, Louisiana.

Ryu, C., Shin, D. and Choi, S., 1999. Bed combustion and gas flow model for MSW incinerator. *Int. J. of Computer Application in Technology*.

Saeed, M. O., Hassan, M. N., and Abdul Mujeebu, M., 2008. Development of Municipal Solid Waste Generation and Recyclable Components Rate of Kuala Lumpur: Perspective Study.

Saidur, R., Abdelaziz, E.A., Demirbas, A., Hossain, M.S. and Mekhilef, S., 2011. A review on biomass as a fuel for boilers. *Renewable and Sustainable Energy Reviews 15,* 2262–2289.

Sivapalan Kathiravale, Mohamad Puad Abu, Muhd. Noor Muhd. Yunus, Kamarul Zaman Abd Kadir, 2003. Predicting the Quality of the Refuse Derived Fuel from the Characteristics of the Municipal Solid Waste. *Proceedings of the 2nd Conference on Energy Technology towards a Clean Environment,* Phuket, Thailand.

Sun, Gong-Gang, De-Fu Che and Zuo-He Chi, 2012. Effects of Secondary Air on Flow, Combustion, and NOx Emission from a Novel Pulverized Coal Burner for Industrial Boilers. *Energy Fuels, 26*, 6640−6650.

Swithenbank, J., Nassezadeh, V., Goh, R. and Siddall, R.G., 1999. Fundamental Principles of Incinerator Design. Dev. *Chem. Eng. Mineral Process., 7(5/6),* 623-640.

Won Yang, Donghoon Shin and Sangmin Choi, 1998. A process simulation model for a 2 ton/hr incinerator (A combined bed combustion and furnace heat transfer model). *International Journal of Energy Research, 22 (11),* 943-951.

Yang, Y.B., Sharifi, V.N. and Swithenbank, J., 2004. Effect of Air Flow Rate and Fuel Moisture on the Burning Behaviours of Biomass and Simulated Municipal Solid Wastes in Packed Beds. *Fuel 83,* 1553-1563.

Yang, Y.B., Goh, Y.R., Zakaria, R., Nasserzadeh, V. and Switheńbank J., 2002. Mathematical modelling of MSW incineration on a travelling bed. *Waste Management 22,* 369–380.

Zainura Zainon Noor, Rafiu Olasunkanmi Yusuf, Ahmad Halilu Abba, Mohd Ariffin Abu Hassan, Mohd Fadhil Mohd Din, 2013. An overview for energy recovery from municipal solid wastes (MSW) in Malaysia scenario. *Renewable and Sustainable Energy Reviews 20,* 378–384.